Relativistic many-body calculations of electric-dipole matrix elements, lifetimes, and polarizabilities in rubidium

M. S. Safronova, Carl J. Williams, and Charles W. Clark
Physics Laboratory, National Institute of Standards and Technology, Technology Administration, U.S. Department of Commerce, Gaithersburg, Maryland 20899-8410, USA
(Received 9 July 2003; published 27 February 2004)

Electric-dipole matrix elements for ns-$n'p$, nd-$n'p$, and $6d-4f$ transitions in Rb are calculated using a relativistic all-order method. A third-order calculation is also carried out for these matrix elements to evaluate the importance of the high-order many-body perturbation theory contributions. The all-order matrix elements are used to evaluate lifetimes of ns and np levels with $n=6,7,8$ and nd levels with $n=4,5,6$ for comparison with experiment and to provide benchmark values for these lifetimes. The dynamic polarizabilities are calculated for ns states of rubidium. The resulting lifetime and polarizability values are compared with available theory and experiment.

DOI: 10.1103/PhysRevA.69.022509 PACS number(s): 31.10.+z, 32.10.Dk, 32.70.Jz, 32.80.Rm

I. INTRODUCTION

A recent proposal [1] for quantum computation utilizes the ground hyperfine states of a neutral atom as qubits, and realizes two-qubit quantum gates by conditional excitations to Rydberg states. The atoms are confined to the sites of an optical lattice, and the optical potential seen by the atom depends on the dynamic polarizability of the atom. Therefore, the atom will generally move in a different lattice potential when it is excited to the Rydberg state during the gate operation, which may cause motional heating and lead to decoherence. In a recent paper [2], we proposed two solutions to this problem by matching the ac polarizabilities of the atom in the ground and Rydberg states. In the first scheme, the polarizabilities are matched for the specific values of the lattice photon frequency between the resonances. In the second scheme, some accidental matches between transition energies are used to match the ground-state polarizability with the polarizability of the selected Rydberg states ($11p$ and $15p$ in the case of Rb). The elimination of motional decoherence is important in helping to design a high-fidelity two-qubit gate capable of meeting the error threshold for scalable quantum computation.

Despite the existence of high-precision measurements of the primary transition electric-dipole matrix elements in alkali-metal atoms, accurate experimental data for other transitions are lacking with the exception of a very few transitions in Cs owing to the study of parity nonconservation. In light of the importance of the atomic calculations for the quantum logic gate scheme with conditional excitations to Rydberg levels, we have calculated the electric-dipole matrix elements for subsequent evaluation of lifetimes and polarizabilities for a number of Rb levels. We note that the interest in this particular logic gate scheme with neutral atoms results from its potential for fast (submicrosecond) gate operations.

We have performed all-order calculations of the $7s$-np, $8s$-np, $4d$-np, $5d$-np, and $6d$-np electric-dipole matrix elements with $n=5,6,7$, and 8, and of the $6d$-$4f$ matrix elements. These results are combined with previous all-order calculations of the $5s$-np and $6s$-np matrix elements [3] to obtain values of the lifetimes of the $6s$, $7s$, $8s$, $6p$, $7p$, $8p$, $4d$, $5d$, and $6d$ levels. The lifetime of the $6d_{3/2}$ level is of special interest owing to the large discrepancies between existing experiments [4,5]. The third-order matrix-element calculation has also been carried out to evaluate the importance of the higher-order contributions. The dynamic polarizabilities of the Rb ns states are also calculated for both low-lying and Rydberg levels. The evaluation of the accuracy of the polarizability calculations is conducted including a comparison between our data and other theory and experiment.

II. ELECTRIC-DIPOLE MATRIX ELEMENTS

The electric-dipole matrix elements for the $5s$-$5p$ transitions were measured to high accuracy in Ref. [6] and matrix elements for ns-$n'p$ transitions with $n=5,6$ and $n'=5,6,7,8$ were calculated using a single-double (SD) all-order method in Refs. [3,7]. In the present work, we have calculated matrix elements for $7s$-np, $8s$-np, $4d$-np, $5d$-np, and $6d$-np transitions with $n=5,6,7$, and 8 as well as $4f$-$6d$ transitions using SD all-order method [8]. Very briefly, the wave function is represented as an expansion

$$|\Psi_v\rangle=\left[1+\sum_{ma}\rho_{ma}a_m^\dagger a_a+\frac{1}{2}\sum_{mnab}\rho_{mnab}a_m^\dagger a_n^\dagger a_b a_a+\sum_{m\neq v}\rho_{mv}a_m^\dagger a_v+\sum_{mna}\rho_{mnva}a_m^\dagger a_n^\dagger a_a a_v\right]|\Phi_v\rangle, \tag{1}$$

where Φ_v is the lowest-order atomic state function, which is taken to be the *frozen-core* Dirac-Hartree-Fock (DHF) wave function of a state v; $a_i^\dagger$ and a_i are creation and annihilation operators, respectively. The index a is used to represent core states and indices m and n indicate excited states.

The quantities ρ_{ma} and ρ_{mv} are single core and valence excitation coefficients, and the quantities ρ_{mnab} and ρ_{mnva} are double core and valence excitation coefficients, respectively. We obtain the equations for the excitation coefficients by substituting the above wave function into the many-body

TABLE I. Absolute values of all-order SD electric-dipole matrix elements for the np-$n's$ transitions in Rb in atomic units. The lowest-order (DHF) and third-order values all also given. All-order values for $5s$-np and $6s$-np transitions are from Ref. [3]. The corresponding reduced oscillator strengths are given in rows labeled *f*. All-order matrix elements and experimental energies are used in calculation of oscillator strengths.

	$5s$-$5p_{1/2}$	$5s$-$6p_{1/2}$	$5s$-$7p_{1/2}$	$5s$-$8p_{1/2}$	$5s$-$5p_{3/2}$	$5s$-$6p_{3/2}$	$5s$-$7p_{3/2}$	$5s$-$8p_{3/2}$
DHF	4.819	0.383	0.142	0.078	6.807	0.606	0.237	0.136
Third order	4.181	0.363	0.130	0.069	5.899	0.583	0.224	0.125
All order	4.221	0.333	0.115	0.059	5.956	0.541	0.202	0.111
$f_{5s\to np}$	0.3404	0.0040	0.0006	0.0002	0.6905	0.0106	0.0017	0.0006
	$6s$-$5p_{1/2}$	$6s$-$6p_{1/2}$	$6s$-$7p_{1/2}$	$6s$-$8p_{1/2}$	$6s$-$5p_{3/2}$	$6s$-$6p_{3/2}$	$6s$-$7p_{3/2}$	$6s$-$8p_{3/2}$
DHF	4.256	10.286	0.976	0.375	6.187	14.457	1.498	0.597
Third order	4.189	9.584	1.050	0.420	6.115	13.447	1.610	0.668
All order	4.119	9.684	0.999	0.393	6.013	13.592	1.540	0.628
$f_{6s\to np}$	−0.1946	0.5101	0.0117	0.0023	−0.4019	1.0267	0.0279	0.0058
	$7s$-$5p_{1/2}$	$7s$-$6p_{1/2}$	$7s$-$7p_{1/2}$	$7s$-$8p_{1/2}$	$7s$-$5p_{3/2}$	$7s$-$6p_{3/2}$	$7s$-$7p_{3/2}$	$7s$-$8p_{3/2}$
DHF	0.981	9.360	17.612	1.801	1.393	13.552	24.708	2.728
Third order	0.952	9.304	16.679	1.944	1.347	13.517	23.349	2.943
All order	0.954	9.189	16.844	1.865	1.352	13.353	23.587	2.833
$f_{7s\to np}$	−0.0190	−0.3330	0.6565	0.0186	−0.0375	−0.6821	1.3170	0.0432
	$8s$-$5p_{1/2}$	$8s$-$6p_{1/2}$	$8s$-$7p_{1/2}$	$8s$-$8p_{1/2}$	$8s$-$5p_{3/2}$	$8s$-$6p_{3/2}$	$8s$-$7p_{3/2}$	$8s$-$8p_{3/2}$
DHF	0.514	1.922	16.151	26.817	0.727	2.705	23.343	37.577
Third order	0.500	1.839	16.162	25.587	0.705	2.578	23.428	35.770
All order	0.504	1.853	15.982	25.831	0.710	2.600	23.171	36.123
$f_{8s\to np}$	−0.0063	−0.0278	−0.4701	0.7987	−0.0124	−0.0539	−0.9595	1.5993

Schrödinger equation. The equations are solved iteratively and the resulting expansion coefficients are used to calculate matrix elements. In such a procedure, certain classes of many-body perturbation theory (MBPT) terms are summed to all orders. However, the restriction of the expansion (1) to the single and double excitations leads to some missing terms in the expression for the matrix elements starting from the fourth order. As it is important to understand how significant higher-order corrections are for the transitions under consideration, we also conduct separate third-order calculation of these matrix elements [including random-phase approximation (RPA) contributions iterated to all orders]. The third-order calculation follows that of Ref. [9]. Such a calculation is of lower accuracy than the all-order one but the difference in third-order and all-order values provides an estimate of the importance of the higher-order contributions. Also, the breakdown of both all-order and third-order calculations to different contributions yields information regarding relative importance of the specific terms and possible large cancellations between different terms. Such information can be used to approximate some of the omitted contributions and further estimate the uncertainty of the all-order calculation. We should note that despite the fact that the entire third-order contribution is contained in the all-order result, the extraction of the third-order part from the all-order calculation is not a straightforward task (see Ref. [7] for the correspondence of the terms), so a separate calculation is made to obtain third-order values. The separate calculation also allows us to iterate RPA contribution to all orders.

The all-order and third-order calculations are conducted with a complete set of basis DHF wave functions generated using the *B*-spline method [10]. We use 40 splines of order $k=7$ for each angular momentum. The basis set orbitals are defined on a nonlinear grid and constrained to a large spherical cavity of a radius $R=100$ a.u. This cavity radius is chosen to accommodate all valence orbitals for which atomic properties are being calculated, i.e., all ns, $np_{1/2}$, and $np_{3/2}$ orbitals with $n=5,6,7,8$, $nd_{3/2}$, and $nd_{5/2}$ orbitals with $n=4,5,6$, and $4f_{5/2}$, $4f_{7/2}$ orbitals. The choice of the number of splines, cavity radius, and number of grid points is based on the comparison of the resulting basis set energies of the valence orbitals listed above and electric-dipole matrix elements between these states with the energies and matrix elements resulting from direct numerical solutions of the DHF equations. We require that these basis set energies were accurate to five or more significant figures. We have also verified that the differences between the third-order results obtained with this basis set and more accurate 50 spline basis set are negligible at the current level of accuracy.

We use the system of atomic units, a.u., in which e, m_e, $4\pi\epsilon_0$ and the reduced Planck constant $\hbar$ have the numerical value 1. Polarizability in atomic units has the dimensions of volume, and its numerical values presented here are thus measured in units of a_0^3, where $a_0 \approx 0.052\,918$ nm is Bohr radius. The atomic units for α can be be converted to SI units via $\alpha/h[\mathrm{Hz}/(\mathrm{V/m})^2] = 2.48832\times10^{-8}\alpha(\mathrm{a.u.})$, where the conversion coefficient is $4\pi\epsilon_0 a_0^3/h$ and Planck constant h is factored out. The atomic unit of frequency ω is $E_h/\hbar \approx 4.1341\times10^{16}$ Hz, where E_h is Hartree energy.

The third-order and all-order results for ns-$n'p$ transitions with $n,n'=5,6,7$ and 8 are summarized in Table I to-

TABLE II. Absolute values of all-order SD electric-dipole matrix elements for the np-$n'd$ and $6d$-$4f$ transitions in Rb in atomic units. The lowest-order and third-order values are also given. In the cases where lowest order and SD data are of different sign relative signs are shown.

n	5	6	7	8
		$4d_{3/2}-np_{1/2}$		
DHF	9.046	6.725	1.181	0.578
Third order	8.092	5.289	1.119	0.566
All order	7.847	4.717	1.054	0.541
		$4d_{3/2}-np_{3/2}$		
DHF	4.082	2.955	0.534	0.262
Third order	3.655	2.307	0.502	0.255
All order	3.540	2.055	0.470	0.242
		$4d_{5/2}-np_{3/2}$		
DHF	12.241	8.829	1.601	0.787
Third order	10.964	6.915	1.505	0.764
All order	10.634	6.184	1.411	0.726
		$5d_{3/2}-np_{1/2}$		
DHF	0.244	18.701	13.639	2.660
Third order	1.220	18.241	10.600	2.573
All order	1.616	18.106	9.768	2.400
		$5d_{3/2}-np_{3/2}$		
DHF	0.157	8.443	5.983	1.198
Third order	0.607	8.232	4.609	1.146
All order	0.787	8.160	4.242	1.064
		$5d_{5/2}-np_{3/2}$		
DHF	0.493	25.340	17.884	3.592
Third order	1.821	24.695	13.843	3.435
All order	2.334	24.491	12.798	3.201
		$6d_{3/2}-np_{1/2}$		
DHF	0.512	−0.254	31.349	22.584
Third order	1.076	1.375	31.563	17.647
All order	1.180	1.989	31.422	16.631
		$6d_{3/2}-np_{3/2}$		
DHF	0.255	−0.028	14.158	9.901
Third order	0.513	0.732	14.242	7.662
All order	0.558	1.012	14.161	7.215
		$6d_{3/2}-np_{3/2}$		
DHF	0.778	−0.047	42.500	29.603
Third order	1.532	2.184	42.709	23.041
All order	1.658	2.974	42.481	21.784
	$6d_{3/2}-4f_{5/2}$	$6d_{5/2}-4f_{5/2}$	$6d_{5/2}-4f_{7/2}$	
DHF	6.109	1.642	7.343	
Third order	9.150	2.443	10.924	
All order	9.938	2.642	11.813	

gether with the lowest-order DHF values. The corresponding reduced oscillator strengths calculated using formula [11]

$$f_{ab} = -\frac{30.3756}{(2j_a+1)\lambda}|\langle a\|D\|b\rangle|^2 \qquad (2)$$

are listed in the rows labeled $f_{ns\to n'p}$. In Eq. (2), D is the dipole operator and λ is a transition wavelength in nm. The all-order matrix elements and experimental energies from Ref. [12] are used in the oscillator strength calculation. The sum of the $f_{5s\to np}$ oscillator strengths with $n=5,6,7,8$ slightly exceeds one because the contributions to the sum rule $\Sigma_n f_{5s\to np}=1$ from the transitions with $n=2,3,4$ are negative.

The results for the nd-$n'p$ matrix elements with $n=4,5,6$ and the $n'=5,6,7,8$ and $6d$-$4f$ matrix elements are summarized in Table II. The transitions containing the fine structure components, such as ns-$5p_{1/2}$ and ns-$5p_{3/2}$ pairs, for example, have very similar relative correlation contributions so we will omit the angular momentum j subscript in

TABLE III. Contributions to third-order and all-order electric-dipole reduced matrix elements (a.u.) for selected transitions in Rb.

	$5s$-$5p_{1/2}$	$5s$-$7p_{1/2}$	$7s$-$5p_{1/2}$	$7s$-$7p_{1/2}$	$5d_{3/2}$-$5p_{1/2}$	$5d_{3/2}$-$7p_{1/2}$	$6d_{3/2}$-$6p_{1/2}$	$6d_{3/2}$-$4f_{5/2}$
				Third order				
DHF	4.819	0.149	0.981	17.612	0.244	13.639	−0.254	6.109
RPA	−0.213	−0.060	0.015	−0.024	0.101	0.030	0.045	0.002
BO	−0.419	0.040	−0.038	−0.899	0.888	−3.048	1.589	3.041
SR	0.027	0.009	−0.004	0.002	−0.013	−0.004	−0.005	0.001
Norm	−0.033	−0.001	−0.002	−0.012	−0.001	−0.016	0.000	−0.004
Total	4.181	0.130	0.952	16.679	1.220	10.600	1.375	9.150
				All order				
DHF	4.819	0.142	0.981	17.612	0.244	13.639	−0.254	6.109
Term *a*	−0.234	−0.064	0.014	−0.025	0.102	0.036	0.047	0.005
Term *c*	−0.375	0.009	−0.077	−0.648	1.575	−3.372	2.752	4.393
Term *d*	0.039	0.017	0.056	0.149	−0.197	−0.024	−0.439	−0.089
Other	0.039	0.012	−0.006	0.005	−0.025	−0.004	−0.009	0.002
Norm	−0.068	−0.002	−0.014	−0.248	−0.083	−0.506	−0.109	−0.483
Total	4.220	0.115	0.954	16.844	1.616	9.768	1.989	9.938

the subsequent discussion. We find that the relative correlation correction contribution varies very significantly with the transition. It is small, below 7%, for all $6s$-np, $7s$-np, and $8s$-np transitions and for some nd-$n'p$ transitions. In those situations where the third order and all-order values differ by less than a few percent we expect the dipole matrix elements to be accurate to at least 2%.

We should note that in some cases it is possible that such good agreement of the third-order and all-order values is fortuitous and may result from accurate cancellations of the higher-order terms. We address this issue below in more detail.

In Ref. [3], the all-order values for the primary transitions were found to agree with a recent high-accuracy measurement [6] to within 0.2%–0.35%. The accuracy of the $5s$-$6p$, $5s$-$7p$, and $5s$-$8p$ matrix elements is, however, substantially lower since they are relatively small matrix elements with significant relative correlation contributions. To investigate the correlation contributions in more detail, we give a breakdown of both third-order and all-order calculations for eight selected transitions in Table III. The third-order contributions are separated to RPA, Brueckner-orbital (BO), structural radiation (SR) and normalization corrections following Ref. [9]. For the all-order contributions, three terms (*a*, *c*, and *d*) are listed separately and the other 17 terms are grouped together in row labeled "Other." The derivation and expressions for these terms are given in Refs. [7,8]. A normalization correction is given in row labeled "Norm." As it was noted earlier, there is no straightforward correspondence of the all-order and third-order breakdown (full description is given in Ref. [7]), but term *a* partly corresponds to RPA-like corrections and term *c* to BO-like corrections. Term *d* is normally small with exception of some transitions. It is quadratic in single-valence excitation coefficients ρ_{mv} and, therefore, contains only fifth and higher-order terms. We find strong cancellations between BO and RPA terms for $5s$-$6p$, $5s$-$7p$, and $5s$-$8p$ matrix elements. The difficulty of the calculation of such matrix elements has been described before for the case of Cs [3,13,14]. However, we also find that term *d*, which is missing entirely from third-order calculation is relatively large for $7s$-$5p$ and $7s$-$7p$ matrix elements. It is rather puzzling since we observe very good agreement of third-order and all-order results for these transitions. The possible explanation is accurate cancellation of the high-order terms for these transitions. We note that term *d* is not significant for the $6s$-$5p$ transition, for which some conclusion of accuracy may be drawn from the comparison with similar Cs transition matrix elements (which are measured to quite good accuracy). Accurate measurements of these matrix elements would be very useful in developing further understanding of this issue. We note that even though this term is significant, it is not very large, on the order of 5%.

In the case of nd-$n'p$ transitions, the term *c* (or BO term for third-order calculation) dominates. The relative contribution of the correlation correction varies with the transition. For $5d$-$5p$ and $6d$-$6p$ transitions, the DHF approximation gives a very poor result; the sign of the matrix element changes when correlation is added for $6d$-$6p$ matrix elements and the DHF values for $5d$-$5p$ matrix elements are about seven times too low. As expected, we find very large, 25%–30%, differences between third-order and all-order calculations for these transitions as the all-order calculation includes correlation more completely. The term *c* can be corrected by including triple excitations or use of the semiempirical scaling described in Refs. [3,7,13]. To check the validity of the scaling approach, we applied such a method to the $5d$-$5p$ matrix elements and compared the resulting ratio with the experimental measurement [15].

In Table IV we give our values of the ratio *R*

$$R=\frac{\langle 5p_{3/2}\|D\|5d_{3/2}\rangle}{\langle 5p_{1/2}\|D\|5d_{3/2}\rangle}\frac{\langle 5p_{1/2}\|C_1\|5d_{3/2}\rangle}{\langle 5p_{3/2}\|C_1\|5d_{3/2}\rangle}$$

of the $5p_{3/2}$-$5d_{3/2}$ and $5p_{1/2}$-$5d_{3/2}$ electric-dipole matrix elements divided by the corresponding values of the C_1 reduced matrix elements, where C_1 is the normalized spherical har-

TABLE IV. The ratio R of the $5d_{3/2}-5p_{3/2}$ and $5d_{3/2}-5p_{1/2}$ electric-dipole matrix elements divided by the corresponding values of the C_1 reduced matrix elements, where C_1 is the normalized spherical harmonic. Comparison of the present results calculated in different approximations with theoretical and experimental values from Ref. [15]. The corresponding $5d$-$5p$ matrix elements, divided by the corresponding values of the C_1 reduced matrix elements are also given.

	$5p_J-5d_{J'}$			R
$J-J'$	3/2−5/2	3/2−3/2	1/2−3/2	
DHF	0.3182	0.3034	0.2115	1.434
Third order	1.1756	1.1758	1.0562	1.113
All order	1.5063	1.5248	1.3995	1.089
Scaled	1.2801	1.2882	1.1707	1.100
MBPT [15]	1.0238	1.0216	0.9000	1.135
Expt. [15]				1.068(8)

monic [11]. The present results are compared with theoretical and experimental values from Ref. [15]. The corresponding $5d$-$5p$ matrix elements, divided by the corresponding values of the C_1 reduced matrix elements are also given. The theoretical value of Ref. [15] was obtained using relativistic third-order many-body theory [9]; some higher-order Brueckner-orbital terms were also included, which accounts for the difference with our third-order result. As noted above, the largest contribution to the $5p$-$5d$ matrix elements calculated using the all-order method comes from the term c containing single-valence excitation coefficients ρ_{mv}. We scale these excitation coefficients ρ_{mv} with the ratio of the experimental and corresponding theoretical correlation energies as described in Refs. [3,13]. We list the results obtained using such scaling in a row labeled ''Scaled.'' We find very significant differences between all high-precision calculations, which indicates that the accuracy of the all-order calculation is around 10-20 % for these matrix elements. However, our all-order result for the ratio R is in much better agreement with experiment [15] than the third-order value and theoretical calculation of Ref. [15].

III. LIFETIMES

We use the resulting all-order matrix elements to calculate the lifetimes of the $6s$, $7s$, $8s$, $6p$, $7p$, $8p$, $4d$, $5d$, and $6d$ levels in Rb for the comparison with experiment and providing benchmark values for these lifetimes.

The Einstein A coefficients A_{vw} [11] are calculated using the formula

$$A_{vw}=\frac{2.02613\times 10^{15}}{\lambda^3}\frac{|\langle v\|D\|w\rangle|^2}{2j_v+1}\ \mathrm{s}^{-1}, \tag{3}$$

where $\langle v\|D\|w\rangle$ is the reduced electric-dipole matrix element for the transition between states v and w and λ is corresponding wavelength in nanometers. The lifetime of the state v is calculated as

TABLE V. Transition energies (E/hc) in cm^{-1}, matrix elements (in a.u.) and corresponding contributions to $7p_{3/2}$ radiative width (in MHz).

Transition (vw)	$\langle v\|D\|w\rangle$	δE_{vw}	A_{vw}	$\Sigma_w A_{vw}$
$7p_{3/2}-7s$	23.587	1559	1.068	1.068
$7p_{3/2}-6s$	1.540	7736	0.556	1.624
$7p_{3/2}-5s$	0.202	27870	0.447	2.071
$7p_{3/2}-5d_{3/2}$	4.242	2169	0.093	2.164
$7p_{3/2}-4d_{3/2}$	0.470	8515	0.069	2.234
$7p_{3/2}-5d_{5/2}$	12.798	2169	0.847	3.081
$7p_{3/2}-4d_{5/2}$	1.411	8515	0.623	3.703

$$\tau_v=\frac{1}{\sum_w A_{vw}} \tag{4}$$

and the denominator of Eq. (4) gives the radiative width of the level v.

Several electric-dipole (E1) transitions contribute to the lifetime of each of the levels considered here. The simplest case is that of the $6s$ level, where only $6s$-$5p_{1/2}$ and $6s$-$5p_{3/2}$ transitions need to be included. To calculate the lifetime of the $8p_{3/2}$ state, we need to include ten E1 transitions and in the case of the $6d_{3/2}$ level seven E1 transitions are allowed, including the $6d_{3/2}$-$4f_{5/2}$ transition. The experimental energies from Ref. [12] are used in the lifetime calculation. We illustrate the importance of the different channels contributing to the lifetime of the $7p_{3/2}$ state in Table V, where we give the coefficients A_{vw} for each transition together with the transition energies from [12] and corresponding matrix elements from Tables I and II. The accumulated sum $\Sigma_w A_{vw}$ is listed in the last column. We find the contribution from the $7p_{3/2}$-$5d_{5/2}$ transition to be nearly as large as the contribution from the $7p_{3/2}$-$7s$ transition. All seven contributions need to be included in an accurate calculation. The smallest contribution to $\Sigma_w A_{vw}$ comes from $7p_{3/2}$-$4d_{3/2}$ transition and is around 2%.

We list the contributions to $6d_{3/2}$ and $6d_{5/2}$ lifetimes as well as the corresponding matrix elements and transition energies in Table VI. The dominant contributions to $6d_{3/2}$ and $6d_{5/2}$ lifetimes come from the $6d_{3/2}$-$5p_{1/2}$ and $6d_{5/2}$-$5p_{3/2}$ transitions, respectively. The next largest contribution is 14% for the $6d_{3/2}$ lifetime and 7% for the $6d_{5/2}$ lifetime. We find the contributions from $6d_{3/2}$-$4f_{5/2}$ and $6d_{5/2}$-$4f_{7/2}$ transitions to be around 7% for the corresponding level.

The results for the ns, np, and nd lifetimes obtained using all-order matrix elements are compared with experimental values from Refs. [4,5,16] in Table VII. We omit the effect of the blackbody radiation in our calculations. In Ref. [16], it was estimated to be small for the levels considered here with the exception of the $8p$ levels. It is still far below experimental uncertainty of the $8p$ level lifetime. The results agree with experiment within the experimental precision for $6s$, $7s$, $8s$, $6p$, and $4d$ levels. The values of the $7p$, $8p$, $5d$, and $6d$ lifetimes are in good agreement with experiment. The lower accuracy of the calculations is expected for these

TABLE VI. Transition energies E/hc in cm^{-1}, matrix elements (a.u.) and the corresponding contributions to $6d_{3/2}$ and $6d_{5/2}$ radiative widths (in MHz).

Transition (vw)	$\langle v\|D\|w\rangle$	δE_{vw}	A_{vw}	$\Sigma_w A_{vw}$
$6d_{3/2}-5p_{1/2}$	1.180	16108	2.948	2.948
$6d_{3/2}-6p_{1/2}$	1.989	4972	0.246	3.194
$6d_{3/2}-7p_{1/2}$	31.422	852	0.309	3.504
$6d_{3/2}-5p_{3/2}$	0.558	15870	0.630	4.134
$6d_{3/2}-6p_{3/2}$	1.012	4894	0.061	4.195
$6d_{3/2}-7p_{3/2}$	14.161	817	0.055	4.250
$6d_{3/2}-4f_{5/2}$	9.938	1895	0.341	4.591
$6d_{5/2}-5p_{3/2}$	1.658	15872	3.712	3.712
$6d_{5/2}-6p_{3/2}$	2.974	4896	0.351	4.063
$6d_{5/2}-7p_{3/2}$	42.481	819	0.335	4.398
$6d_{5/2}-4f_{5/2}$	2.642	1897	0.016	4.414
$6d_{5/2}-4f_{7/2}$	11.813	1897	0.322	4.736

levels owing to the lower accuracy of the np-$n'd$ matrix elements with comparison to most of the np-$n's$ ones due to large correlation corrections for these matrix elements. It should be noted that the experimental uncertainties of $7p$, $8p$, and $5d$ lifetimes are rather large (up to 20%) and two recent experiments for the $6d_{3/2}$ level give substantially different values: 256(4) ns and 298(8) ns. Our result for $6d_{3/2}$ lifetime (263 ns) is very close to the first measurement, however, large uncertainties in the correlation contributions to the relevant transitions do not allow to rule out 10% larger value of this lifetime.

TABLE VII. Radiative widths (MHz) and lifetimes (ns) for ns, np, and nd states in Rb. Experimental values are taken from the compilation in Ref. [16] unless noted otherwise. The lifetimes obtained using *ab initio* all-order matrix elements and scaled all-order values are listed in columns τ_v and τ_v^{sc}, respectively.

State	$\Sigma_w A_{vw}$	τ_v	τ_v^{sc}	τ_v^{expt}	
$6s$	21.761	46.0	45.4	46(5)	
$7s$	11.318	88.4	88.3	88(6)	
				91(11)	
$8s$	6.201	161.3	161.8	161(3)	[4]
				154(7)	
				153(8)	
$6p_{1/2}$	7.729	129	123	125(4)	
				131(5)	
$7p_{1/2}$	3.394	295	280	272(15)	
$8p_{1/2}$	1.899	527	508		
$6p_{3/2}$	8.461	118	113	112(3)	
$7p_{3/2}$	3.703	270	258	246(10)	
				233(10)	
$8p_{3/2}$	2.056	486	471	400(80)	
$4d_{3/2}$	11.478	87	83.5	86(6)	
$5d_{3/2}$	5.193	193	243	205(40)	
$6d_{3/2}$	4.591	218	263	256(4)	[4]
				298(8)	[5]
$4d_{5/2}$	10.674	94	90	94(6)	
$5d_{5/2}$	5.340	187	235	230(23)	
$6d_{5/2}$	4.736	211	252	249(5)	[4]

The accuracy of the theoretical calculations for these levels may be improved by including some triple-excitation contributions into the corresponding wave functions.

We estimate some omitted higher-order contributions using the scaling of the single excitation coefficients ρ_{mv} described above. The contributions containing these single-excitation coefficients are dominant for all of the transitions needed for the calculation of lifetimes in Table VII. The lifetimes obtained using scaled all-order matrix elements are listed in column τ_v^{sc}. We find that the scaled data agree with experimental values within the experimental uncertainty for all levels with exception of $7p_{3/2}$ and $6d_{3/2}$, where the theoretical values are just outside the experimental uncertainties.

IV. POLARIZABILITIES

The valence part of the ac polarizability of an alkali-metal atom in ns state can be calculated using the formula

$$\alpha_v^{ns}(\omega)=\frac{1}{3}\sum_{n'}\left(\frac{(E_{n'p_{1/2}}-E_{ns})\langle n'p_{1/2}\|D\|ns\rangle^2}{(E_{n'p_{1/2}}-E_{ns})^2-\omega^2}+\frac{(E_{n'p_{3/2}}-E_{ns})\langle n'p_{3/2}\|D\|ns\rangle^2}{(E_{n'p_{3/2}}-E_{ns})^2-\omega^2}\right), \quad (5)$$

where D is the dipole operator. In this formula, ω is assumed to be at least several linewidths off resonance with the corresponding transition.

The core contribution to the polarizability, calculated in the DHF approximation is found to be small for Rb ($9.3\ a_0^3$) and is weakly dependent on ω in the frequency range considered here. The static value for the polarizability of Rb^+ calculated in the random-phase approximation [17,18] is $9.1a_0^3$, close to the value of $9.0a_0^3$ obtained by Johansson [19] from analysis of the observed term values of nonpenetrating Rydberg states. The accuracy of the RPA approximation for the core polarizability is estimated to be 5% in Ref. [3]. We use the RPA value for the core polarizability of Rb^+ as a baseline, and adjust it to account for valence electron [using Eq. (5) with $n'=2,3,4$] and the frequency dependence by using DHF calculations. The RPA and DHF values differ by only 2 %. The correction to the core polarizability owing to the presence of the valence electron is very small, it is only $-0.3a_0^3$ for $5s$ state in DHF approximation.

First, we describe the calculation of the ground-state polarizability $\alpha_{5s}(\omega)$. The expression (5) converges rapidly with n' so the contribution with $n'=5$ is dominant. We use experimental $5s$-$5p$ matrix elements from Ref. [6], all-order matrix elements from Ref. [3], and experimental energies from [12] to evaluate the expression of Eq. (5) with $n'=5,6,7,8$. The contribution to the ground-state polarizability from states with $n'>8$ is very small, $0.2a_0^3$ in DHF approximation. We plot the ground state frequency-dependent polar-

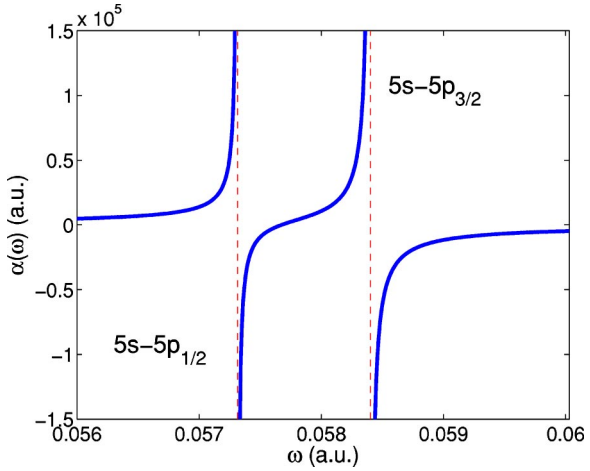

FIG. 1. Dynamic polarizability $\alpha(\omega)$ for the ground state of Rb in atomic units.

izability in the vicinity of the $5s$-$5p_{1/2}$ and $5s$-$5p_{3/2}$ resonances in Fig. 1. The behavior within the few linewidths from the resonances is not shown and the exact placement of the resonances is indicated by the vertical dashed lines. As we see from Fig. 1, $\alpha_{5s}(\omega)$ changes sign between two resonances. We determined that $\alpha_{5s}(\omega)=0$ at $\lambda_{vac}=790.032(8)$ nm [2], where the uncertainty results from the uncertainty of the polarizability calculation. This crossing point is of interest for the optical lattice experiments with Rb as the atoms will no longer be trapped at this wavelength.

We give the breakdown of the different contributions to the ground state polarizability for one particular frequency, $\omega=0.04298$ a.u., corresponding to $\lambda=1.06$ μm [20], in Table VIII. The comparison with other theory [21] and experiment [22] is also given. Our value is in good agreement with the result from [21]. The discrepancy is due to our use of more accurate values for the electric-dipole matrix elements. Our result is just outside the range of uncertainty of the value $\alpha=(769\pm61)a_0^3$ inferred by Bonin and Kadar-Kallen from an atomic deflection experiment [22].

Next, we describe the calculation of the polarizabilities of the Rydberg states. We calculate the polarizabilities of the ns

TABLE VIII. Contributions to ground-state dynamic polarizability of Rb in a_0^3 for $\omega=0.04298$ a.u.

	Contribution	Value
	$n'=5$	682.84
	$n'=6$	1.48
	$n'=7$	0.16
	$n'=8$	0.04
	$\alpha_v(n'=5..8)$	684.52(72)
	$\alpha_v(n'>8)$	0.17(8)
	$\alpha_{vc}(n'=2.4)$	−0.26(13)
	α_c	9.10(45)
Final α		693.5(9)
Ref. [21]		711.4
Expt. [22]		769(61)

TABLE IX. Dynamic polarizabilities $\alpha_{ns}(\omega)$ (in units of a_0^3) for Rb, $\omega=0.0576645$ a.u., i.e. $\lambda=790$ nm.

n	$\alpha_{\rm DHF}$	α	n	$\alpha_{\rm DHF}$
8	−304	−295[a]	14	−286
9	−292		15	−285
10	−289		16	−284
11	−288		17	−282
12	−287		18	−280
13	−287		19	−277

[a]High-accuracy value obtained using experimental energies and all-order matrix elements for the dominant terms with $n'=7,8$.

states of Rb with $n=8$ . . . 19 using the DHF approximation; i.e., using DHF values for both energies and matrix elements in Eq. (5). We note that the calculations of the Rydberg state polarizabilities are done with actual DHF states which are direct numerical solutions of the DHF equations. We do not employ the B-spline basis set technique in the Rydberg state polarizability calculations as the cavity radius which would be required to accommodate $n=20$ states is too large to reproduce the wave functions of the relevant states even when large (100 spline) basis set is used.

The DHF calculations are done on the nonlinear grid of the form

$$r(i)=r_0(e^{(i-1)h}-1). \tag{6}$$

To calculate matrix elements and energies of the first few excited states 500 grid points are sufficient. This type of grid provides a very dense grid near the origin. Thus we needed to confirm that there were sufficient points at large R to support the Rydberg states. The parameters r_0 and h were chosen to ensure sufficient number of points to calculate $\langle ns\|D\|n'p\rangle$ matrix elements for high values of n and n'. However, we found that the accurate DHF values of the matrix elements even between high Rydberg states can be obtained with relatively small number of grid points. For example, the values of the $20s$-$20p_{3/2}$ matrix element obtained with 500 and 40 000 point grids (corresponding to approximately 10 and 200 points in the relevant grid section) differ by only 0.05%. The summation over n' in Eq. (5) is truncated at $n'=23$ for all of the states. Such truncation is justified owing to very fast convergence of the sum over n' in Eq. (5) [2]. To verify that the contributions from higher n' and continuum are not significant at the present level of accuracy we conduct separate calculation of the polarizability of the $10s$ state using B-spline basis set. We verified that the result is independent on the cavity radius, when it is large enough to accommodate $n=10$ and $n=11$ s and p orbitals; we used cavities from 200 to 450 a.u.. The summation over the entire basis set yields the result −292 a.u. which differs from the value in Table IX by only 1 %.

To evaluate the accuracy of the DHF approximation we also calculate the $8s$ polarizability using the all-order matrix elements from Table I. We find DHF result to be in good agreement with the high-precision value. The results of the DHF calculation for $\omega=0.0576645$ a.u. corresponding to λ

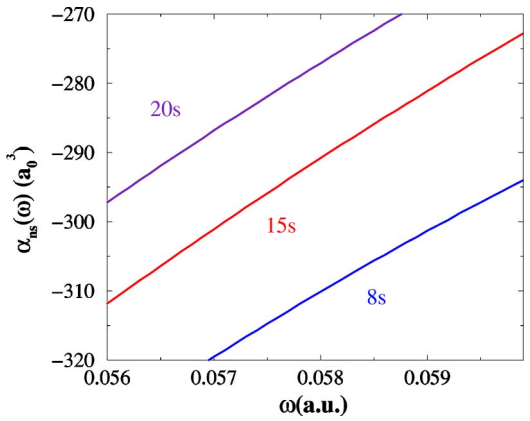

FIG. 2. Dynamic polarizability $\alpha(\omega)$ for the ns states of Rb in a_0^3.

$=790$ nm as well as high-precision calculation for $n=8$ are given in Table IX. We find that the polarizability values do not change substantially with n for $n>8$.

We plot the frequency-dependent polarizabilities of $8s$, $15s$, and $20s$ states in Fig. 2. As expected, the polarizabilities depend weakly on ω for the frequencies considered here. The polarizabilities of the ground and Rydberg states can be matched at the point between two resonances where the ground-state polarizability is small and negative. The exact matching point for the $15s$ state is $\lambda_{vac}=790.14(2)$ nm [2]. The matching of the polarizabilities allows to minimize motional heating in the quantum computation scheme with neutral atoms.

V. CONCLUSION

We have conducted a systematic study of the ns-$n'p$ and nd-$n'p$ electric-dipole matrix elements in rubidium using relativistic all-order method. An investigation of the accuracy of these matrix elements was performed. The resulting matrix elements were used to calculate lifetimes of the ns and np levels with $n=6,7,8$, and nd levels with $n=4,5,6$. The lifetime values were found to be in good agreement with experiment. The dynamic polarizabilities of the ns Rb states, which are of interest for the optimization of quantum computation scheme with neutral atoms mediated by the conditional excitations to Rydberg states, were also calculated.

ACKNOWLEDGMENTS

This work was partially supported by the Advanced Research Development Activity, the National Security Agency, and NIST Advanced Technology Program.

[1] D. Jaksch, J.I. Cirac, P. Zoller, S.L. Rolston, R. Côté, and M.D. Lukin, Phys. Rev. Lett. **85**, 2208 (2000).
[2] M.S. Safronova, C.J. Williams, and C.W. Clark, Phys. Rev. A **67**, 040303 (2003).
[3] M.S. Safronova, W.R. Johnson, and A. Derevianko, Phys. Rev. A **60**, 4476 (1999).
[4] A. Ekers, A. Głódź, J. Szonert, B. Bieniak, K. Fronc, and T. Radelitski, Eur. Phys. J. D **8**, 49 (2000).
[5] W.A. van Wijngaarden and J. Sagle, Phys. Rev. A **45**, 1502 (1992).
[6] U. Volz and H. Schmoranzer, Phys. Scr., T **65**, 48 (1996).
[7] M.S. Safronova, Ph.D. thesis, University of Notre Dame, 2000 (unpublished).
[8] S.A. Blundell, W.R. Johnson, Z.W. Liu, and J. Sapirstein, Phys. Rev. A **40**, 2233 (1989).
[9] W.R. Johnson, Z.W. Lui, and J. Sapirstein, At. Data Nucl. Data Tables **64**, 279 (1996).
[10] W.R. Johnson, S.A. Blundell, and J. Sapirstein, Phys. Rev. A **37**, 307 (1988).
[11] W.R. Johnson, *Lecture Notes on Atomic Physics*, http://www.nd.edu/~johnson.
[12] C.E. Moore, *Atomic Energy Levels*, Natl. Bur. Stand. Ref. Data Ser. 35 (U.S. GPO, Washington, D.C., 1971), Vol. II, p. 180.
[13] S.A. Blundell, W.R. Johnson, and J. Sapirstein, Phys. Rev. A **43**, 3407 (1991).
[14] A.A. Vasilyev, I.M. Savukov, M.S. Safronova, and H.G. Berry, Phys. Rev. A **66**, 020101 (2002).
[15] S.B. Bayram, M. Havey, M. Rosu, A. Sieradzan, A. Derevianko, and W.R. Johnson, Phys. Rev. A **61**, 050502(R) (2000).
[16] C.E. Theodosiou, Phys. Rev. A **30**, 2881 (1984).
[17] A. Derevianko, W.R. Johnson, M.S. Safronova, and J.F. Babb, Phys. Rev. Lett. **82**, 3589 (1999).
[18] W.R. Johnson, D. Kolb, and K.-N. Huang, At. Data Nucl. Data Tables **28**, 333 (1983).
[19] I. Johansson, Ark. Fys. **20**, 135 (1961).
[20] We use the value $\omega=0.04298$ a. u. that was used in Ref. [21], but we note that the value $\omega=0.04281$ a.u. actually corresponds to the wavelength in air of $\lambda=1.064$ μm of the Nd:YAG laser.
[21] M. Marinescu, H.R. Sadeghpour, and A. Dalgarno, Phys. Rev. A **49**, 5103 (1994).
[22] K.D. Bonin and M.A. Kadar-Kallen, Phys. Rev. A **47**, 944 (1993).